IEEE Access
Multidisciplinary | Rapid Review | Open Access Journal

Received 28 December 2022, accepted 12 January 2023, date of publication 16 January 2023, date of current version 25 January 2023.

Digital Object Identifier 10.1109/ACCESS.2023.3237591

RESEARCH ARTICLE

A Dispatchable Droop Control Method for PV Systems in DC Microgrids

JIAHUA NI[1,2], BO ZHAO[3], (Member, IEEE), ARMAN GOUDARZI[1], YANJUN LI[4], AND JI XIANG[1,2], (Senior Member, IEEE)

[1]College of Electrical Engineering, Zhejiang University, Hangzhou 310027, China
[2]Huzhou Institute of Zhejiang University, Huzhou 313000, China
[3]The Electric Power Research Institute State Grid Zhejiang Electric Power Company Ltd., Hangzhou 310027, China
[4]Zhejiang University City College, Hangzhou 310027, China

Corresponding author: Ji Xiang (jxiang@zju.edu.cn)

This work was supported in part by the National Natural Science Foundation of China under Grant 61773339 and Grant 62073290.

ABSTRACT Along with the sustained growth of photovoltaic (PV) penetration, the PV generation is expected to be more active in DC microgrids rather than maximum power generation. The droop control methods are generally adopted to achieve power regulation at steady-state and passive power-sharing at transient state. However, the traditional $V-I$ droop based control methods can not realize voltage dispatch orders and require mode switching to prevent overload problem which increases control complexity and deteriorate the performance. To address this issue, this paper proposes a novel dispatchable droop control method. The proposed method utilizes a two-layer hierarchical control structure. The primary layer is $V-dp/dv$ droop control to achieve passive power-sharing at a smaller time scale. The secondary layer realizes power or voltage regulation based on the dispatch orders at a larger time scale. Moreover, with the dp/dv as the control variable, the proposed method realizes seamless mode switching and has the ability to roughly indicate the power margin of PVs, which is critical for dispatching PVs. Several case scenarios are conducted in hardware-in-loop tests to validate the feasibility and effectiveness of the proposed control strategy on DC microgrids.

INDEX TERMS PV system, dispatchable, hierarchical control, $V-dp/dv$ droop control, DC microgrids.

I. INTRODUCTION

The photovoltaic (PV) generation offers a number of advantages such as clean green energy production (zero-emission), noise-free power generation, zero-fuel cost, diverse applications, low maintenance cost, smart energy networks suitability, etc. These factors make PV generation one of the most attractive renewable energies to replace fossil fuel-based generations [1]. Moreover, the DC nature of PV is more efficiently exploited with DC microgrids (DCMGs) as most modern electronic loads require DC power which decreases the energy loss compared to AC microgrids [2]. Hence, the PV is usually an essential part of the emerging DCMGs, and the PV generations' power control is crucial in DCMGs operation [3].

The associate editor coordinating the review of this manuscript and approving it for publication was Gab-Su Seo.

Conventionally, the PV generation is regarded as an undispatchable unit due to its intermittent and randomness and is expected to operate in maximum power point tracking (MPPT) mode to maximize the economic benefits [4], [5]. The energy storage and fuel generator are dispatched to minimize the power loss and operation cost [6]. However, with the increase of PV penetration, it is not always the optimal solution to set the PV generation in MPPT mode since the investment and maintenance cost is also increasing to smooth the PVs' power fluctuation. Thus, in a sense, the PVs is more suitable to be dispatched as variable capacity sources to prevent the frequent charge and discharge of energy storage to prolong its lifetime [7], [8].

The researchers have proposed several strategies to achieve power regulation actively. In [9], [10], and [11], the authors introduce power reserve control methods to curtail a specific amount power of PVs. The generated power is equal to the

This work is licensed under a Creative Commons Attribution 4.0 License. For more information, see https://creativecommons.org/licenses/by/4.0/

available power minus the reserved power. However, these methods can not achieve dispatched power regulation since the generated power varies with the environmental factors. The constant power generation algorithms are presented in [12] and [13] to realize dispatched power regulation. As long as the available power is greater than the dispatched power, the output power will keep at the dispatched power regardless of environmental changes. However, these methods are always used in the PV power plants connected to the utility grid.

The droop control method is preferable when the PV generation is operated in the microgrid. The droop control mimics the inertia characteristic as synchronous generator, which achieves power-sharing and plug-and-play functionalities [14]. However, it lacks the ability of specific power and voltage regulation. Thus, the researchers are committed to modifying droop control scheme to achieve specific control objectives.

Power sharing improvement is a hot topic of droop control modification. In [15], a piecewise linear formation is proposed to adaptively set droop gain with the deviation of bus voltage. In [16], a nonlinear droop curve is designed to choose the droop coefficient with output current. Reference [17] introduces a two-layer control scheme, which adds an integral term of output power to the primary droop control layer, and a voltage restoration coefficient is assigned through a secondary low-bandwidth layer. Reference [18] defines a factor to converge to the average value and modifies the output voltage reference with a unique voltage-shift term. Reference [19] minimizes the power losses with a multiobjective optimization-based intelligent computation approach to derive the optimal droop coefficients. Reference [20] uses harmony search (HM) and partial swarm optimization (PSO) techniques to find the optimal droop parameters. However, these methods focus on the power sharing accuracy and can not achieve dispatching orders.

Power regulation is another hot topic of droop control modification. In [21], a droop control based hierarchical scheme is proposed to fulfill the economic dispatch order. The droop character is shifted along the power axis by addition of a current reference from the economic regulator. In addition, a voltage correction term is added in order to cancel out the effect of line impedance. In [22], a proportional-integral (PI) controller derives adaptive voltage terms to achieve zero-error power regulation. In [23], a virtual voltage axis is utilized to coordinate the traditional droop control and DC bus signaling to minimize the voltage deviation and enable power regulation. Three operation bands are defined to determine the compensation voltage term. However, these methods assume that the desired power is realizable and ignore the uncertainty of PVs' capacities. Reference [24] considers the maximum power of renewable energy generators. The setpoint of droop control is updated according to the upper layer optimization algorithm to realize power regulation. However, a voltage restoration module is usually combine with the power regulation. In the steady state, the PV system generates the dispatched power, and the output voltage will be restored to near the rated value, but the specific value is determined by the power flow and impedances of the network, lacking the ability to realize voltage dispatching.

Moreover, the above-mentioned droop control algorithms are based on the traditional $V-I$ or $V-P$ droop scheme. Ultimately, the voltage reference is generated, and the inner control loop achieves the reference value tracking. However, the voltage reference may be unrealizable due to the insufficient of PVs' capacities, which may be caused by the mismatch in dispatch orders or the sharp drop in PVs' capacities. The traditional dispatchable methods usually utilize inner control modification or extra equipments to prevent overload issue. Reference [25] introduces an integrated power control (IPC) module which takes hill climbing method as inner loop to adaptively switch the output mode. Reference [26] and [27] design mode switching modules to trigger MPPT when PV capacity is insufficient. Reference [28] and [29] invest energy storages to deal with the power shortage. However, there methods increases the control complexity or investment cost.

In [30], a droop concept establishes the relationship between dp/dv and bus voltage deviation. It utilizes the dp/dv reference to regulate the PV power and does not need mode switching. Given the advantage of dp/dv regulation, this paper proposes a dp/dv based dispatchable droop control method, which combines the droop scheme and power/voltage regulation. The proposed method utilizes a two-layer hierarchical control structure to achieve different control objectives at different time scale. The primary layer is $V-dp/dv$ droop control to achieve power-sharing at the smaller time scale. The secondary layer is to realize power regulation or voltage control to modify the rated dp/dv value at the larger time scale.

A. STATEMENT OF CONTRIBUTIONS

The proposed method is a modified $V-dp/dv$ droop control method based on [30]. Compared to the $V-dp/dv$ droop control in [30] and the existing droop control based methods, the proposed method brings two major benefits: First, the modified $V-dp/dv$ droop control method is dispatchable to realize dispatch orders, which is unachievable in [30]; Second, the proposed method offers two dispatchable modes, that are power mode and voltage mode, which can achieve more flexible and accurate dispatch functionality.

B. ORGANIZATION

The rest of this paper is organized as follows: Section II illustrates the PV's characteristics. In Section III, the PV's dispatchable concept and mechanism are presented. Section IV elaborates the proposed method. Section V analyses the small-signal stability of the proposed method. Hardware-in-loop tests to validate the proposed method's feasibility and effectiveness are performed in Section VI, and Section VII concludes the paper.

II. PV's CHARACTERISTICS

The mathematic model of an ideal PV array current is given by [31] and [32]

$$i_{pv} = N_p\left[I_{sc,n} - I_{0,n}\left(exp(\frac{v_{pv}}{N_s a V_t}) - 1\right)\right]. \quad (1)$$

Here, i_{pv} and v_{pv} are the PV output current and voltage; N_p and N_s are the numbers of parallel- and series-connected PV modules and each of modules is composed of N PV cells; $I_{sc,n}$ is the short-circuit current of the PV module; $I_{0,n}$ is the reverse saturation or leakage current of the diode; $V_t = NKT/q$ is thermal voltage with q being the electron charge, a being the diode ideality constant and K being the Boltzmann constant; T is the temperature of the p-n junction of the diode.

The output power of the PV array is given by

$$p_{pv} = N_p v_{pv}\left[I_{sc,n} - I_{0,n}\left(exp(\frac{v_{pv}}{N_s a V_t}) - 1\right)\right]. \quad (2)$$

Then, the derivative of power versus voltage is

$$\frac{dp}{dv} = N_p\left[(I_{sc,n} + I_{0,n}) - I_{0,n}(1 + \frac{v_{pv}}{N_s a V_t})exp(\frac{v_{pv}}{N_s a V_t})\right]. \quad (3)$$

And the terminal values of dp/dv are

$$\begin{cases} \left.\frac{dp}{dv}\right|_{v_{pv}=0} = N_p I_{sc,n} > 0 \\ \left.\frac{dp}{dv}\right|_{v_{pv}=U_{oc}} = -N_p I_{0,n}\frac{U_{oc}}{N_s a V_t} exp(\frac{U_{oc}}{N_s a V_t}) < 0. \end{cases} \quad (4)$$

Thus, there is a point $v_{pv} = U_{mp}$ where $dp/dv = 0$ and the output power is maximum $p_{pv} = P_{max}$. At the open-circuit voltage, U_{oc}, the value of dp/dv is minimum which can be regard as constant [30]:

$$(dp/dv)^{min} \approx -\frac{\overline{I}_{sc}\overline{U}_{oc}}{N_s a \overline{V}_t}, \quad (5)$$

where $\overline{I}_{sc}, \overline{U}_{oc}, \overline{V}_t$ are short circuit current, open circuit voltage and thermal voltage at nominal condition $(1000W/m^2, 298.16K)$.

Fig. 1 illustrates the characteristic curves of a PV array composed of KC200GT modules [31]. Fig. 1 (a) is the $P-V$ curve which can be divided into two segments, that is uphill part and the downhill part. Meanwhile, the $P-dp/dv$ curve, shown in Fig. 1 (b), can be split into two parts that is $dp/dv < 0$ and $dp/dv > 0$ corresponding to the $P-V$ curve. The point at $dp/dv = 0$ is always the maximum power point (MPP) regardless of the variation of irradiation and temperature, and the right side of MPP on $P-V$ curve is corresponding to the left side of MPP on $P-dp/dv$ curve, and vice versa [30]. Moreover, comparing the two regions on each curve, one draws the principle that the changing rate of power to voltage is greater at downhill part and the operation range of dp/dv is wider at $dp/dv < 0$ part. Thus, it is recommended to take the downhill ($dp/dv < 0$) part as operating scope for better performance of dynamic and steady response. This paper is based on this principle and realizes the power/voltage regulation by controlling the dp/dv value of PV.

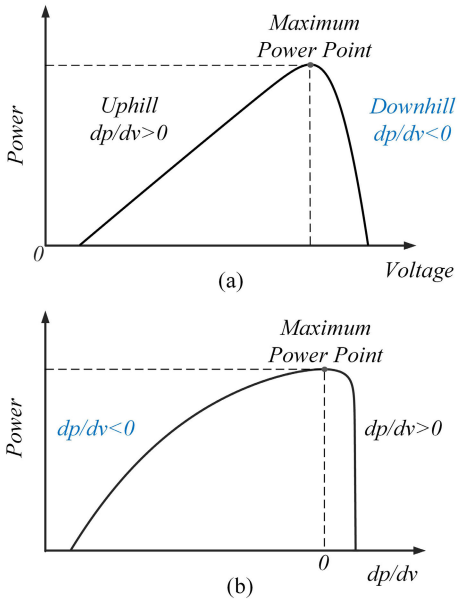

FIGURE 1. Curves of a PV array. (a) $P-V$ curve. (b) $P-dp/dv$ curve.

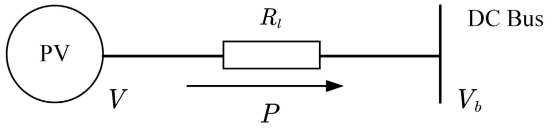

FIGURE 2. Equivalent circuit of PV generation connected to a common DC bus.

III. PV's DISPATCHABLE FUNDAMENTALS

A. DISPATCHABLE CONCEPT

This paper proposes a dispatchable droop control structure for PV generations in DC microgrids. The PV generation can be dispatched in power regulation mode or voltage control mode. As illustrated in Fig. 2, the power delivered from the PV generation can be expressed as

$$P = (V - V_b)^2/R_l, \quad (6)$$

where P is output power, V is output voltage, R_l is line impedance and V_b is DC bus voltage.

That is, with the fixed DC bus voltage V_b and line impedance R_l, the generated power P can be uniquely determined if the output voltage V is set and vice versa. Thus, the PV generation can only be operated in one mode at a time:

P mode: dispatched with a power reference to achieve power regulation.

V mode: dispatched with a voltage reference to achieve voltage control.

B. DISPATCHABLE MECHANISM

Traditionally, the $V-I$ droop scheme is utilized as primary control to maintain the power balance with source/load transient and modified by a secondary layer to regulate the distributed generator (DG)'s output power.

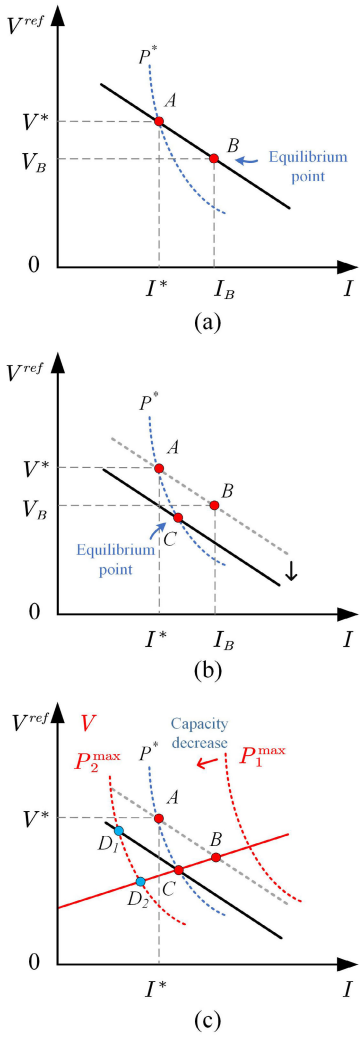

FIGURE 3. Diagram of droop control modification. (a) Traditional droop control curve. (b) Modified droop control curve. (c) Droop control curve under different PV's capacities.

The modified droop control equation can be expressed as [20]

$$V^{ref} = V^* - R(I - I^*) + \delta V, \tag{7}$$

where V^{ref} is voltage reference of DG's output, R is droop coefficient, V^* and I^* are the nominal values of voltage and current, I is the output current, and δV is the modification value. As shown in Fig. 3 (a), the point B is the solution based on the droop scheme and the power balance of the microgrid, which usually deviates the nominal power P^*, the blue dashed curve. By adding a modification value δV, the droop curve shifts along the voltage axis, as shown in Fig. 3 (b). With the changing of droop curve, the equilibrium point of DG is also moving along the droop curve. The modifying process stops when the equilibrium point stables at point C, where the output power restores to nominal value P^*, thereby realizing the dispatchable of DG.

The modified $V-I$ droop control methods usually assume that demanded power can be supplied by the DG. This may not be true for PVs with intermittency and uncertainty caused by environmental changes. The power deficiency will cause overload problem. As illustrated in Fig. 3 (c), the red dashed curves represent the PV's equal power curves, whose left area is feasible area, and the red curve represents the relationship between DG's output voltage and power derived from Eq. (6). When the PV has enough capacity, $P_1^{max} > P^*$, the DG will stable at equilibrium point C, which means the droop scheme is achievable under output characteristic constraint. Then, the PV's capacity drops form P_1^{max} to P_2^{max} under sudden irradiance reduction. According to the droop scheme, the equilibrium point is point D_1. While the equilibrium point is supposed to be point D_2 based on output characteristic constraint. This conflict makes the droop scheme no longer achievable. A nature solution is to change the operation mode into MPPT when overload problem occurs. However, the mode switch increases the control complexity and deteriorates the performance.

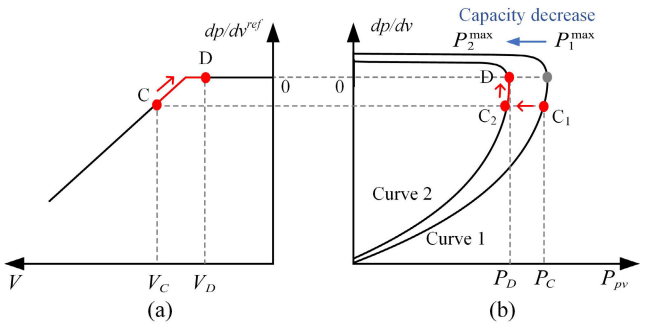

FIGURE 4. $V-dp/dv$ droop curve interacts with PV's $P-dp/dv$ characteristic curves.

The $V-dp/dv$ droop control scheme is a better option for PV generation since it avoids overload problem with seamless mode switch. The control scheme can be expressed as [30]

$$\frac{dp}{dv}^{ref} = \frac{dp}{dv}^* - m(V - V^*), \quad \frac{dp}{dv}^{ref} \le 0, \tag{8}$$

where $(dp/dv)^{ref}$ means the reference of dp/dv, $(dp/dv)^*$ is the nominal value of dp/dv, m is droop coefficient and V^* is the nominal voltage. As shown in Fig. 4 (a), the reference of dp/dv is generated based on the output voltage of DG. And the DG's output power is equal to the power generated from PV. Supposing that point C is the equilibrium point when the PV's characteristic curve is curve 1, where $P_C < P_1^{max}$. Then, the PV's characteristic curve drops from curve 1 to curve 2 under sudden irradiance reduction similar to the condition in $V-I$ droop control. The PV's operating point changes from point C_1 to point C_2 at first. And the output voltage of DG will decrease with power deficiency, which leads to the increase of the reference of dp/dv based on the droop scheme. Since the reference of dp/dv will hold at maximum value zero which means the PV's maximum power point regardless the decreasing output voltage. Finally, the DG will stable at an new equilibrium point D, where satisfies the output characteristic as $P_2^{max} = (V_D - V_b)^2/R_l$. This mechanism naturally

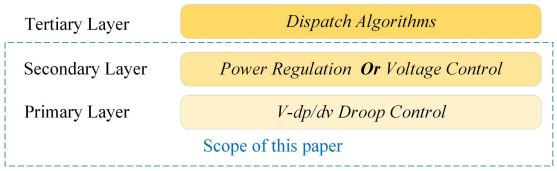

FIGURE 5. Diagram of proposed hierarchical control structure.

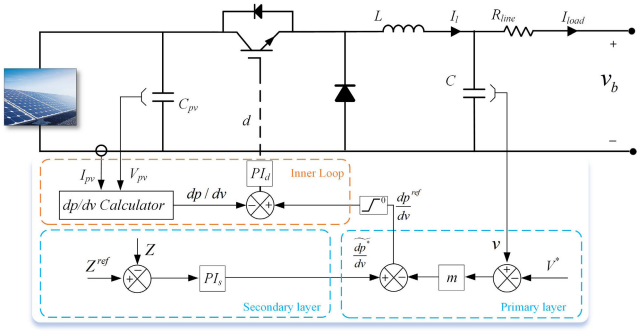

FIGURE 6. PV generation system under proposed control scheme.

avoids the overload problem and enhances the robust of PV generation.

Therefore, the $V-dp/dv$ droop control is more suitable for PV generation considering the PVs' intermittency and uncertainty. However, the $V-dp/dv$ droop control only realizes power sharing and can not achieve voltage/power dispatching of PVs. Inspired by the modified $V-I$ droop control method, the dispatching of PV generation can be transferred into the modifying of $V-dp/dv$ droop control.

IV. THE PROPOSED DISPATCHABLE DROOP CONTROL METHOD

The proposed dispatchable droop control method, which adopts the hierarchical control structure, consists of two layers: the primary layer is $V-dp/dv$ droop control scheme to share the load passively; the secondary layer is power regulation or voltage control to obey the order from the higher layer. As shown in Fig. 5, the control layers in the blue dash box is the scope of the proposed method. The tertiary layer can be any economic dispatching algorithms to give dispatch orders, which is beyond the scope of this paper.

Fig. 6 shows a typical PV generation system with the proposed hierarchical controller. The buck converter shown in the figure is intended to provide a case study for the following analysis. The control structure consists of the inner and outer control loop. The inner control loop, drawn in the orange dashed box, is to regulate the PV's dp/dv value according to the reference from the outer control loop. The outer control loop, depicted in the blue dashed box, is the proposed control scheme illustrated as follows.

A. THE PRIMARY CONTROL LAYER

The function of this layer is to share the power passively when load changes. Traditionally, the $V-I$ droop is utilized to adjust DG's output current according to the voltage deviation to achieve power sharing. However, since the overload issue as described in Section III. The $V-dp/dv$ droop control establishes the relationship between voltage deviation and PV's dp/dv value. As illustrated in Section II, there is a non-linear correspondence between the output power and dp/dv value regardless of capacity: zero stands for maximum power and then power decreases as dp/dv value decrease. The PV's $P-dp/dv$ characteristic inherently protect the system from overload issue since the maximum value of dp/dv is fixed at zero. Thus, we adopt the $V-dp/dv$ droop control [30] as the primary layer. The control scheme can be written as follows:

$$\frac{dp^{ref}}{dv} = \widetilde{\frac{dp^*}{dv}} - m(V - V^*), \quad \frac{dp^{ref}}{dv} \leq 0, \tag{9}$$

where $\widetilde{dp/dv}^*$ is the modified nominal value generated in secondary control layer.

And m is a fixed value based on PV's capacity indexed by dp/dv:

$$m = \frac{(dp/dv)^{min}}{V^{max} - V^{min}}, \tag{10}$$

where V^{max}, V^{min} are the upper and bottom voltage boundary of the microgrid.

B. THE SECONDARY CONTROL LAYER

The function of this layer is to realize the dispatch order from the tertiary layer. There are two dispatch modes: P mode and V mode. The P mode regulates the output power of PV generation and the V mode controls the output voltage. Thus, the PI controller is utilized to achieve zero-error tracking. The control scheme is given as follows:

$$\widetilde{\frac{dp^*}{dv}} = K_{ps}(Z^{ref} - Z) + K_{is}\int_{-\infty}^{t}(Z^{ref} - Z)d\tau, \tag{11}$$

where K_{ps} and K_{is} are the proportional and integral gains of the compensator, which are related to the timescale of the secondary layer and designed in the next section; $Z \in \{P, V\}$, is the output power or voltage value; $Z^{ref} \in \{P^{ref}, V^{ref}\}$, is the reference of power or voltage from a higher layer.

The modified nominal dp/dv value will increase/decrease until the error decreases to zero. However, the error may never get to zero when the dispatch orders beyond the capacities of PVs. Although the dp/dv reference is limited at zero, the outcome of the integrator will increase to be windup. Therefore, an anti-windup control structure should be added to protect the integrator [33].

Taking dp/dv as the control variable not only brings the benefits of anti-overload mentioned in Section III-B, but also has the advantage that the output value of dp/dv can be used as a rough index to measure the PV's power margin. As illustrated in Section II, the dp/dv and output power have an intrinsic mapping relationship. The operating range of dp/dv is fixed at $[(dp/dv)^{min}, 0]$ corresponding to the output power range of PV, $[0, P_{max}]$, and P_{max} is affected by environmental factors. Therefore, in the proposed method, the PV's power

margin can be roughly indicated according to the margin between dp/dv and 0. While in the traditional algorithm based on $V-I$ droop control, it is difficult to indicate the PV's power margin by the output power or voltage value.

Remark: *The proposed hierarchical control structure is different from the traditional ones. The traditional hierarchical control structure usually can be divided into three layers: droop control as the primary layer, voltage restoration as the secondary layer and power regulation as the tertiary layer [34]. In the steady state, the tertiary layer is in the dominant, and the generator outputs the specified power. The generator's output voltage will be restored to a value near the rated value, but its specific voltage value, determined by the power flow and line impedance, is uncertain. However, the proposed hierarchical control structure separates the voltage control and power regulation into different modes to offer a more flexible way to dispatch the PVs. The generator's output voltage can be accurately dispatched in the V mode, which is preferable for nodes with voltage-sensitive buses.*

V. SMALL-SIGNAL ANALYSIS AND PARAMETERS DESIGN

This section mainly investigates the stability of a PV generation when it operates in the P mode. The dynamic characteristics of the PV array and buck converter are included to evaluate the integrated closed-loop stability of the proposed control strategy.

A. PV MODELING

The linearized small-signal PV model is described by the line tangent to the I-V curve, Eq. (1), around the operating point (i_{pv}, v_{pv}) as given by

$$\Delta i_{pv} = K_{pv}\Delta v_{pv}. \tag{12}$$

with

$$K_{pv} = -\frac{N_p I_{sc,n}}{[exp(V_{oc,n}/aV_t)-1]aN_sV_t}\cdot exp(\frac{v_{pv}}{aN_sV_t}), \tag{13}$$

where $V_{oc,n}$ is the open-circuit voltage of PV module, $V_t = NkT/q$ is the thermal voltage of a PV module.

Then, taking Eq. (12) into account, the perturbation of dp/dv can be derived as given:

$$\Delta\frac{dp}{dv} = K_{pv}\Delta v_{pv} + \Delta i_{pv} = 2K_{pv}\Delta v_{pv} \tag{14}$$

B. CONVERTER MODELING

As for the system illustrated in Fig. 6, the average variable model of the buck converter is given as follows:

$$L\frac{di_l}{dt} = v_{pv}\cdot d - v_b \tag{15}$$

$$C\frac{dv_b}{dt} = i_l - i_{load} \tag{16}$$

$$C_{pv}\frac{dv_{pv}}{dt} = i_{pv} - i_l\cdot d \tag{17}$$

where L is the inductance of the converter inductor, C is the capacitance of converter output capacitor and C_{pv} is the capacitance of converters input-side capacitor. Here, v is the capacitor voltage, i_l is the inductor current, i_{load} is the load current and d is the duty ratio of the buck converter.

Then, the small-signal dynamics of the buck converter is made by perturbing the averaged variables around the operating point:

$$L\frac{d\Delta i_l}{dt} = V_{pv}\cdot\Delta d + D\cdot\Delta v_{pv} - \Delta v_b \tag{18}$$

$$C\frac{d\Delta v_b}{dt} = \Delta i_l - \Delta i_{load} \tag{19}$$

$$C_{pv}\frac{d\Delta v_{pv}}{dt} = K_{pv}\cdot\Delta v_{pv} - D\cdot\Delta i_l - I_l\cdot\Delta d \tag{20}$$

The DC steady period values are capitalized and small signals are marked with a Delta sign.

C. CONTROLLER MODELING

As depicted in Fig. 6, the controller can be divided into two parts, the inner dp/dv regulator in the orange dashed box and the outer proposed dispatchable droop control method in the blue dashed box.

For the inner loop, the control model can be expressed as:

$$d = (\frac{dp}{dv}^{ref} - \frac{dp}{dv})\cdot(K_{pd} + K_{id}/s). \tag{21}$$

where K_{pd}, K_{id} are the compensator's proportional and integral gain, respectively.

Then, the small-signal model of the inner dp/dv regulator can be derived as follows [30]:

$$\Delta d = (\Delta\frac{dp}{dv}^{ref} - 2K_{pv}\cdot\Delta v_{pv})\cdot K_{pd} + \Delta\gamma. \tag{22}$$

Here $\Delta\gamma$ is the perturbation of the integral output, which is given as follows:

$$\frac{d\Delta\gamma}{dt} = (\Delta\frac{dp}{dv}^{ref} - 2K_{pv}\cdot\Delta v_{pv})\cdot K_{id}, \tag{23}$$

For the outer loop, linearizing Eq. (9) and Eq. (11) and written in Laplace form, the small-signal of the outer control scheme is derived as follows:

$$\begin{aligned} s\Delta\frac{dp}{dv}^{ref} &= -(sK_{ps}+K_{is})V_b\Delta i_{load} + (sK_{ps}+K_{is})\Delta P^{ref} \\ &\quad -[s(K_{ps}I_{load}+m)+K_{is}I_{load}]\Delta v_b. \end{aligned} \tag{24}$$

D. SYSTEM ANALYSIS

Combing (14)-(24), the state-space model of the PV system can be derived as

$$\begin{aligned} \dot{X} &= A\cdot X + B\cdot U \\ X &= [\Delta i_l \quad \Delta v_b \quad \Delta v_{pv} \quad \Delta\frac{dp}{dv}^{ref} \quad \Delta\gamma]^T \\ U &= [\Delta i_{load} \quad s\Delta i_{load} \quad \Delta P^{ref} \quad s\Delta P^{ref}]^T, \end{aligned} \tag{25}$$

where A represents system matrix, and B is the input matrix. The system matrix A is given as equation (26), as shown at the bottom of the next page.

TABLE 1. Electrical parameters.

Element Type	Value
Duty Ratio	$D = 0.7$
PV Voltage	$V_{pv} = 571.5V$
PV Current	$I_{pv} = 150.5A$
Inductor Current	$I_l = 215.1A$
Bus Voltage	$V_b = 400.0V$
Slope of I-V Curve	$K_{pv} = -1.09$
Droop Coefficient	$m = 40$

With the electrical parameters in Table. 1 and the PV generator parameters of APOS Energy AP130 in Table. 2, the root loci of the system matrix is analyzed. Fig. 7 (a) shows the first set of root loci with the control parameters set as $K_{is} = 0.01$, and K_{ps} changing from 0 to 0.1. The dominant pole λ_5 shift closer to the imaginary axis which indicates that the system response will become more oscillatory as K_{ps} increases. Fig. 7 (b) follows with another set of root loci obtained with $K_{ps} = 0.001$ and K_{is} varying from 0.001 to 1. Only one pole λ_5 is again found to affect the system dynamics since the other poles are far away from the imaginary axis. The system dynamics is expected to be improved as K_{is} increases.

E. DESIGN OF K_{ps}, K_{is}

According to the analysis above, the small signal model of system is stable within the given PI parameters range. However, the specific control parameters should be designed upon the system performance requirement. Taking the dynamic tracking time of the second layer is equal to T_s as an example, the design is as follows.

Since the bandwidth of the secondary layer is small, and its tracking time is generally long enough to ensure the effect of the primary layer, we can ignore the underlying dp/dv tracking process to have $dp/dv = (dp/dv)^{ref}$. Define the control error as $e = P^{ref} - P$. The small signal control equation can be expressed as

$$\Delta\frac{dp}{dv} = (K_{ps} + \frac{K_{is}}{s})\Delta e. \tag{27}$$

Linear the relationship between dp/dv and P for simplicity as $\Delta dp/dv = K_{pwm}\Delta P$ with $K_{pwm} = (dp/dv)^{min}/P_{pv}^{max}$. Then, equation (27) is transformed into

$$((K_{pwm} + K_{ps})s + K_{is})\Delta e = 0. \tag{28}$$

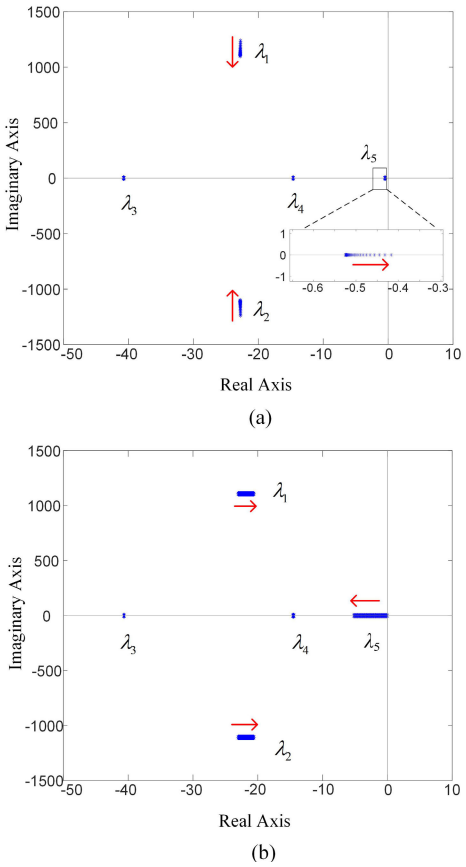

FIGURE 7. Root locus diagram. (a) K_{ps} changes from 0 to 0.1. (b) K_{is} changes from 0.001 to 1.

According to the classical control theory, the time constant of the response is

$$\tau = -K_{is}/(K_{pwm} + K_{ps}). \tag{29}$$

The settling time T_s is taken as four times the time constant. Then, the PI parameters shall meet the following equation

$$-\frac{4K_{is}}{K_{pwm} + K_{ps}} = T_s. \tag{30}$$

For $|K_{pwm}| \gg K_{ps}$ and K_{ps} mainly affect the overshoot, K_{ps} can be set to zero. And K_{is} is set to $-T_sK_{pwm}/4$ to satisfy the dynamic tracking requirements of the secondary layer.

VI. HIL TESTS

To evaluate the performance of the proposed control method, the DC MG system as depicted in Fig. 8 (a) has been studied. The studied system contains a DC load, three different kinds

$$A = \begin{bmatrix} 0 & -\frac{1}{L} & \frac{D-2K_{pv}K_{pd}V_{pv}}{L} & \frac{V_{pv}K_{pd}}{L} & \frac{V_{pv}}{L} \\ \frac{1}{C} & 0 & 0 & 0 & 0 \\ -\frac{D}{C_{pv}} & 0 & \frac{K_{pv}+2K_{pv}K_{pd}I_l}{C_{pv}} & -\frac{I_lK_{pd}}{C_{pv}} & -\frac{I_l}{C_{pv}} \\ -\frac{m+K_{ps}I_{load}}{C} & -K_{is}I_{load} & 0 & 0 & 0 \\ 0 & 0 & -2K_{pv}K_{id} & K_{id} & 0 \end{bmatrix}. \tag{26}$$

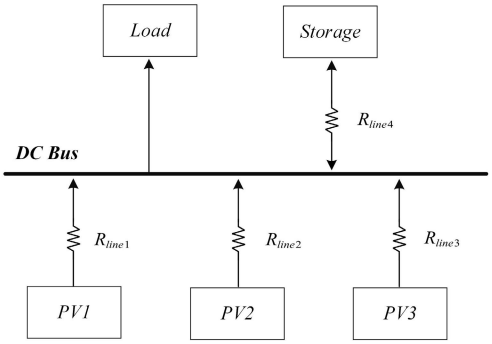

(a)

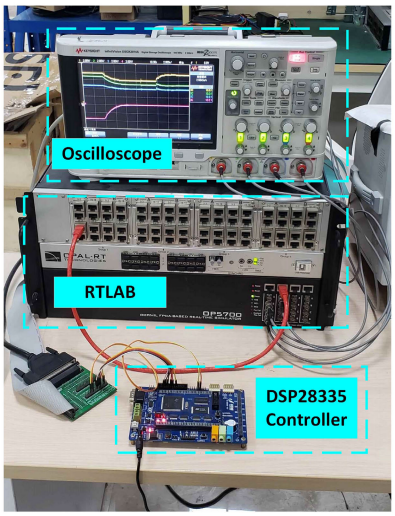

(b)

FIGURE 8. Studied system and HIL tests setup. (a) Studied DC microgrid. (b) HIL tests setup.

of DGs (PV units), and a storage. The DC load is resistive and changeable. Each PV unit has the same structure as Fig. 6, the PV panels are input to the buck converter, and then the converter is connected to the DC bus through a line resistance. The parameters of PV generators are listed in Tab. 2. The energy storage is switchable and its maximum charging and discharging power is 400kW. The power circuits are established in RT-LAB using accurate models and the control system for each PV generation is implemented by external digital signal processor (DSP) chips (TMS320F28335). The equipment of the hardware in loop (HIL) tests is shown in Fig. 8 (b).

The rated DC bus voltage V^* is 400V, whose allowable maximum V^{max} is 440V and minimum V^{min} is 360V. The line resistance between the PV generators and the DC bus is that $R_{line1} = R_{line2} = R_{line3} = 1\ m\Omega$ and the line resistance between the storage and the DC bus is that $R_{line4} = 2\ m\Omega$. The droop coefficients are designed according to Eq. 5, Eq. 10 and parameters presented in Tab. 2, that are -51, -43, -27. The settling time is set as 2s and the parameters of the secondary

TABLE 2. Parameters of PV generators.

Parameter	Kyocera Solar KC200GT	Conergy P180M	APOS Energy AP130
a	1.355	1.304	1.132
N	54	72	36
$I_{sc,n}$	8.21A	5.2A	7.86A
$V_{oc,n}$	32.9V	45V	22.07V
N_p/N_s	40/20	52/15	25/30
P_{mpp}	160 kW	140 kW	96.8 kW
C_{pv}	20 mF	20 mF	20 mF
C	40 mF	40 mF	40 mF
L	10 mH	10 mH	10 mH

layer are designed according to Section V-E, that are $K_{ps} = 0$, $K_{is} = 0.03$.

Two cases are designed to evaluate the performance of the proposed control method. Case 1 is used to test the control effectiveness of the proposed dispatchable droop control method. Case 2 compares the proposed method with the traditional $V - I$ droop based method. Fig. 9 - 11 show the results of tests, which are the screen shots of the oscilloscope. The oscilloscope channel magnitude, time and grounding information are automatically generated with the oscilloscope screen shoots. The oscilloscope channel magnitude and time information are at the top of each figure. For clarifying the real magnitudes of signals, we added an indication of the scale at the lower right corner. Moreover, the grounding information is at the left of the figures, with is marked as T and a grounding sign. The grounding information is out of the scope in voltage subfigure, because the signal is zoom out to clearly show the voltage changes. Thus, we added a reference line of rated voltage V*.

A. CASE STUDY 1: POWER/VOLTAGE DISPATCHING WITH THE PROPOSED METHOD

This case is used to validate the basic functionalities of the proposed dispatchable droop control. The tertiary layer can be distributed control or centralized control algorithms to achieve different operational objectives. Since this case study mainly investigates the control effectiveness of the proposed method, a centralized control method is adopted in the tertiary layer to dispatch the PV generators to realize basic functionalities. The environmental condition is unchanged at $1000W/m^2$, $25°C$, and the capacity of the PV generators are 160kW, 140kW, and 96.8kW, respectively.

As shown in Fig. 9, the test can be divided into four periods. In period I, the PV generators operate in $V-dp/dv$ droop control, and the storage operates in traditional $V - I$ droop control. The load is 0.533 Ω. Then, the power sharing achieves passively according to the droop scheme. The DC bus voltage deviates from the nominal value to 408V. The output power of PV units are 155.5kW, 135.2kW, 94.3kW, respectively. The energy storage is charging at 73kW. In period II, the secondary layer is enabled, and all the PV generators are dispatched to operate in P mode with power references as $120kW$, $100kW$, and $80kW$, respectively. After 4s, all the

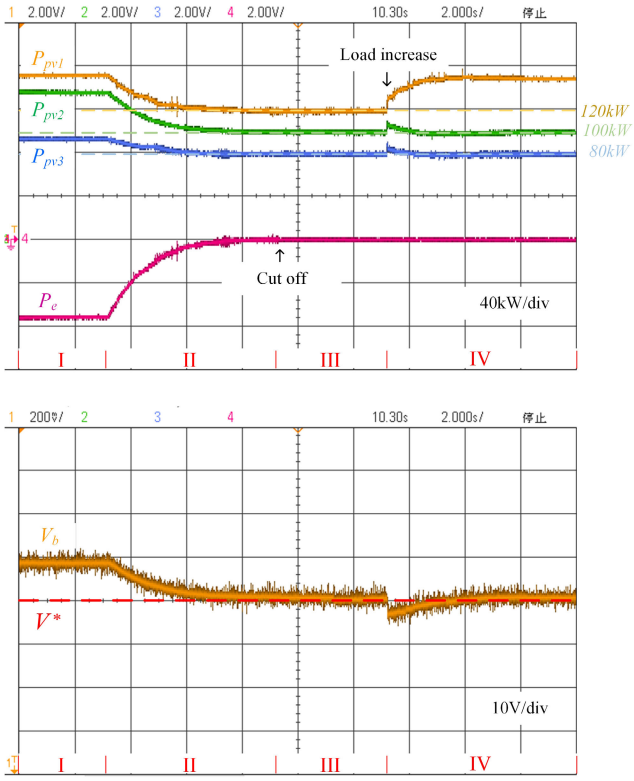

FIGURE 9. Dispatching performance under the proposed control scheme.

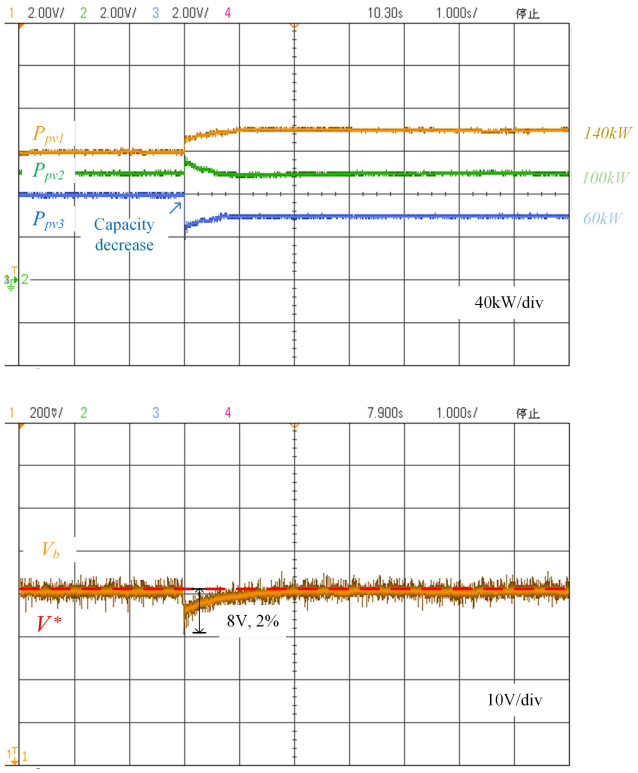

FIGURE 10. Proposed $V - dp/dv$ droop based method.

output power of the PV generators is stable at the reference value. The charging power of storage decreases to zero The voltage restores to rated value 400V. In period III, the storage is cut off to prevent overcharge, and the PV1 generator is chosen to adopt the V mode to keep the bus voltage at the nominal voltage. The output power is unchanged since the DC bus voltage is already stable at the nominal value. In period IV, the load decreases to 0.485 Ω and the load increases by 30kW, which leads to a voltage drop at the initial moment. The increased load is shared between the PV generators due to the primary droop control layer, the output power of PV units are 134kW, 110kW, 86kW, respectively. While, with the effect of the secondary layer, the PV2 and PV3 generators track the old power references, 80kW, 100kW, and the output power of PV1 generator is 150kW to undertakes the extra load to restore the bus voltage.

B. CASE STUDY 2: COMPARISON WITH V – I DROOP BASED METHOD UNDER OVERLOAD ISSUE

The case study is used to verify the proposed method's advantage of overload prevention as illustrated in Section III-B over the traditional $V - I$ droop based method [27]. The test is conducted under the same condition as the period III in case 1, that is the PV1 adopts the V mode, and the PV2 and PV3 adopt the P mode, and the load is 0.533 Ω. At 3s, the capacity of PV3 reduces from 96.8kW to 60kW due to a sudden irradiance drop. Then, the PV3's capacity is no longer enough to realize the 80kW power output.

Fig. 10 shows the performance of the proposed $V - dp/dv$ droop based dispatchable method. The output power of PV3 drops due to the capacity decrease, which leads to the bus voltage drops. At the initial moment, the bus voltage decreases to 382V. The PV1 and PV2 share the load because of $V - dp/dv$ droop control and the output power are 128kW, 112kW, respectively. Under the effect of the secondary layer, the output power of PV2 and PV3 are restored to the old power reference. The PV2 is restored to 100kW, while the PV3 has insufficient capacity to fulfill the old power reference. The PV3's dp/dv reference will increase to the maximum value of 0, and the PV3's output power stables at the maximum power point of 60kW. Ultimately, after 2s, the PV1 undertakes the extra load to restore the bus voltage and generates 140kW.

To have a fair comparison, the PV generators adopt the same control structure but replace the $V - dp/dv$ droop control with $V - I$ droop control as the primary layer. Fig. 11 shows the performance of the traditional $V - I$ droop based method. The output power of PV3 drops sharply due to power deficiency. The PV3 may shut down unless switched to maximum power tracking mode. Thus, a mode switch control structure is added to prevent the overload problem. However, the mode switch increases the control complexity and introduces dynamic oscillation. As portrayed in the figure, the power and voltage oscillate when the mode switches. The voltage oscillation amplitude is up to 28V and the power oscillation amplitudes are 60kW, 40kW, 80kW, respectively. Eventually, the system takes about 6s to settle down.

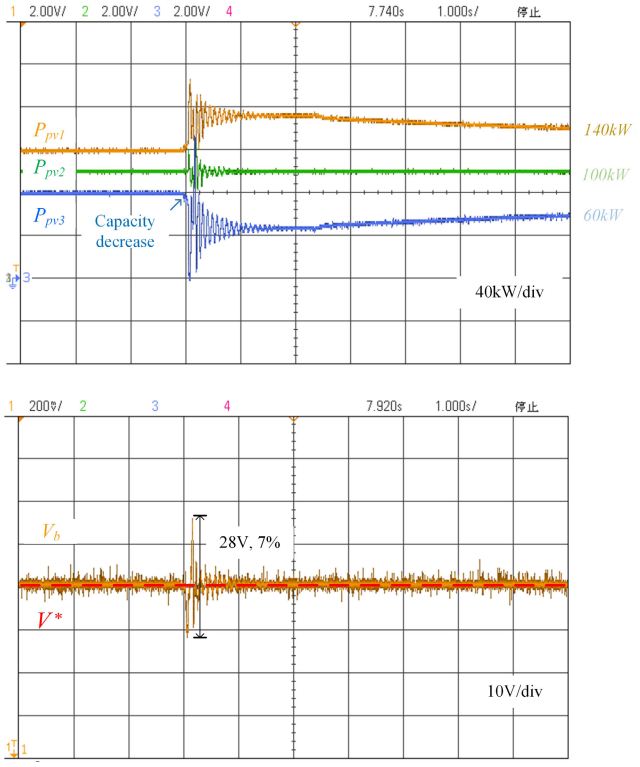

FIGURE 11. Traditional $V-I$ droop based method.

VII. CONCLUSION

A dispatchable droop control method in the DC grid is proposed to cooperate with the economic dispatching of PV systems. The control scheme adopts a hierarchical control structure: the first layer presents droop characteristics to achieve power sharing, and the second layer obeys dispatching instructions. Different from the traditional control method based on $V-I$ droop control, the proposed method is based on $V-dp/dv$ droop control, with dp/dv as the control variable, which not only avoids the overload problem but also uses the value of dp/dv as an index to estimate the PV power margin. Then, the small signal stability of the proposed algorithm is analyzed, and the second layer control parameter design method is given. Finally, the basic dispatching function of the proposed algorithm is tested on the hardware in loop platform and compared with the traditional dispatchable method based on $V-I$ droop control, highlighting the advantages of the proposed dispatching droop control method in overload prevention.

Limitation: The accurate power sharing of the $V-dp/dv$ droop control layer is unavailable. The droop coefficient is fixed and the change of dp/dv is linear to the voltage deviation under the droop characteristics. Since the non-linear relationship between PV's output power and the value of dp/dv, the voltage deviation is non-linear to the output power either. **Future work:** The idea can be extended to be applied in AC grid. The proposed dispatchable droop control method is only suited for the DC grid, for the corresponding relationship between node voltage and power in the DC grid. However, in the AC grid, the frequency and reactive power should be considered. The $V-dp/dv$ droop control is no longer available. Nevertheless, the characteristics of dp/dv is universal. It can be utilized to prevent overload problem and index the power margin in the design of inverter control.

REFERENCES

[1] R. Singh, "Solar-city plans with large-scale energy storage: Metrics to assess the ability to replace fossil-fuel based power," *Sustain. Energy Technol. Assessments*, vol. 44, Apr. 2021, Art. no. 101065.

[2] S. Ullah, A. M. A. Haidar, and H. Zen, "Assessment of technical and financial benefits of AC and DC microgrids based on solar photovoltaic," *Electr. Eng.*, vol. 102, no. 3, pp. 1297–1310, Sep. 2020.

[3] P. J. Dos Santos Neto, T. A. S. Barros, J. P. C. Silveira, E. R. Filho, J. C. Vasquez, and J. M. Guerrero, "Power management techniques for grid-connected DC microgrids: A comparative evaluation," *Appl. Energy*, vol. 269, Jul. 2020, Art. no. 115057.

[4] A. K. Podder, N. K. Roy, and H. R. Pota, "MPPT methods for solar PV systems: A critical review based on tracking nature," *IET Renew. Power Gener.*, vol. 13, no. 10, pp. 1615–1632, Jul. 2019.

[5] R. B. Bollipo, S. Mikkili, and P. K. Bonthagorla, "Critical review on PV MPPT techniques: Classical, intelligent and optimisation," *IET Renew. Power Gener.*, vol. 14, no. 9, pp. 1433–1452, 2020.

[6] C. Li, F. de Bosio, F. Chen, S. K. Chaudhary, J. C. Vasquez, and J. M. Guerrero, "Economic dispatch for operating cost minimization under real-time pricing in droop-controlled DC microgrid," *IEEE J. Emerg. Sel. Topics Power Electron.*, vol. 5, no. 1, pp. 587–595, Mar. 2017.

[7] R. Luthander, D. Lingfors, and J. Widén, "Large-scale integration of photovoltaic power in a distribution grid using power curtailment and energy storage," *Sol. Energy*, vol. 155, pp. 1319–1325, Oct. 2017.

[8] C. Yoon, Y. Park, M. K. Sim, and Y. I. Lee, "A quadratic programming-based power dispatch method for a DC-microgrid," *IEEE Access*, vol. 8, pp. 211924–211936, 2020.

[9] A. Sangwongwanich, Y. Yang, F. Blaabjerg, and D. Sera, "Delta power control strategy for multistring grid-connected PV inverters," *IEEE Trans. Ind. Appl.*, vol. 53, no. 4, pp. 3862–3870, Jul. 2017.

[10] A. Sangwongwanich, Y. Yang, and F. Blaabjerg, "A sensorless power reserve control strategy for two-stage grid-connected PV systems," *IEEE Trans. Power Electron.*, vol. 32, no. 11, pp. 8559–8569, Nov. 2017.

[11] X. Li, H. Wen, Y. Zhu, L. Jiang, Y. Hu, and W. Xiao, "A novel sensorless photovoltaic power reserve control with simple real-time MPP estimation," *IEEE Trans. Power Electron.*, vol. 34, no. 8, pp. 7521–7531, Aug. 2019.

[12] H. D. Tafti, A. Sangwongwanich, Y. Yang, G. Konstantinou, J. Pou, and F. Blaabjerg, "A general algorithm for flexible active power control of photovoltaic systems," in *Proc. IEEE Appl. Power Electron. Conf. Expo. (APEC)*, Mar. 2018, pp. 1115–1121.

[13] H. D. Tafti, A. I. Maswood, G. Konstantinou, J. Pou, and F. Blaabjerg, "A general constant power generation algorithm for photovoltaic systems," *IEEE Trans. Power Electron.*, vol. 33, no. 5, pp. 4088–4101, May 2018.

[14] F. Gao, R. Kang, J. Cao, and T. Yang, "Primary and secondary control in DC microgrids: A review," *J. Mod. Power Syst. Clean Energy*, vol. 7, no. 2, pp. 227–242, 2019.

[15] Y. Lin and W. Xiao, "Novel piecewise linear formation of droop strategy for DC microgrid," *IEEE Trans. Smart Grid*, vol. 10, no. 6, pp. 6747–6755, Nov. 2019.

[16] Y. Zhang, X. Qu, M. Tang, R. Yao, and W. Chen, "Design of nonlinear droop control in DC microgrid for desired voltage regulation and current sharing accuracy," *IEEE J. Emerg. Sel. Topics Circuits Syst.*, vol. 11, no. 1, pp. 168–175, Mar. 2021.

[17] M. Baharizadeh, M. S. Golsorkhi, M. Shahparasti, and M. Savaghebi, "A two-layer control scheme based on *P-V̇* droop characteristic for accurate power sharing and voltage regulation in DC microgrids," *IEEE Trans. Smart Grid*, vol. 12, no. 4, pp. 2776–2787, Jul. 2021.

[18] W. W. A. G. Silva, T. R. Oliveira, and P. F. Donoso-Garcia, "An improved voltage-shifting strategy to attain concomitant accurate power sharing and voltage restoration in droop-controlled DC microgrids," *IEEE Trans. Power Electron.*, vol. 36, no. 2, pp. 2396–2406, Feb. 2021.

[19] A. M. Dissanayake and N. C. Ekneligoda, "Multiobjective optimization of droop-controlled distributed generators in DC microgrids," *IEEE Trans. Ind. Informat.*, vol. 16, no. 4, pp. 2423–2435, Apr. 2020.

[20] M. Mokhtar, M. I. Marei, and A. A. El-Sattar, "Improved current sharing techniques for DC microgrids," *Electr. Power Compon. Syst.*, vol. 46, no. 7, pp. 757–767, Apr. 2018.
[21] J. Hu, J. Duan, H. Ma, and M. Y. Chow, "Distributed adaptive droop control for optimal power dispatch in DC microgrid," *IEEE Trans. Ind. Electron.*, vol. 65, no. 1, pp. 778–789, Jan. 2018.
[22] Y. Jiang, Y. Yang, S.-C. Tan, and S.-Y.-R. Hui, "Distribution power loss mitigation of parallel-connected distributed energy resources in low-voltage DC microgrids using a Lagrange multiplier-based adaptive droop control," *IEEE Trans. Power Electron.*, vol. 36, no. 8, pp. 9105–9118, Aug. 2021.
[23] B.-S. Ko, G.-Y. Lee, K.-Y. Choi, and R.-Y. Kim, "A coordinated droop control method using a virtual voltage axis for power management and voltage restoration of DC microgrids," *IEEE Trans. Ind. Electron.*, vol. 66, no. 11, pp. 9076–9085, Nov. 2019.
[24] J.-O. Lee, Y.-S. Kim, and S.-I. Moon, "Novel supervisory control method for islanded droop-based AC/DC microgrids," *IEEE Trans. Power Syst.*, vol. 34, no. 3, pp. 2140–2151, May 2019.
[25] M. Golla, S. Sankar, K. Chandrasekaran, S. P. Simon, and N. P. Padhy, "An integrated power control module for photovoltaic sources in DC microgrid system," *Int. J. Electr. Power Energy Syst.*, vol. 142, Nov. 2022, Art. no. 108348.
[26] Y. Han, W. Chen, Q. Li, H. Yang, F. Zare, and Y. Zheng, "Two-level energy management strategy for PV-fuel cell-battery-based DC microgrid," *Int. J. Hydrogen Energ.*, vol. 44, no. 35, pp. 19395–19404, Jul. 2019.
[27] Y. Han, H. Yang, Q. Li, W. Chen, F. Zare, and J. M. Guerrero, "Mode-triggered droop method for the decentralized energy management of an islanded hybrid PV/hydrogen/battery DC microgrid," *Energy*, vol. 199, May 2020, Art. no. 117441.
[28] H. Mahmood, D. Michaelson, and J. Jiang, "A power management strategy for PV/battery hybrid systems in islanded microgrids," *IEEE J. Emerg. Sel. Topics Power Electron.*, vol. 2, no. 4, pp. 870–882, Dec. 2014.
[29] X. Han, Y. Liang, Y. Ai, and J. Li, "Economic evaluation of a PV combined energy storage charging station based on cost estimation of second-use batteries," *Energy*, vol. 165, pp. 326–339, Dec. 2018.
[30] H. Cai, J. Xiang, W. Wei, and M. Z. Chen, "$V-dp/dv$ droop control for PV sources in DC microgrids," *IEEE Trans. Power Electron.*, vol. 33, no. 9, pp. 7708–7720, Nov. 2018.
[31] M. G. Villalva, J. R. Gazoli, and E. R. Filho, "Comprehensive approach to modeling and simulation of photovoltaic arrays," *IEEE Trans. Power Electron.*, vol. 24, no. 5, pp. 1198–1208, May 2009.
[32] Y. Mahmoud and E. El-Saadany, "Accuracy improvement of the ideal PV model," *IEEE Trans. Sustain. Energy*, vol. 6, no. 3, pp. 909–911, Jul. 2015.
[33] A. T. Azar and F. E. Serrano, *Design and Modeling of Anti Wind up PID Controllers*. Cham, Switzerland: Springer, 2015, pp. 1–44.
[34] J. M. Guerrero, J. C. Vasquez, J. Matas, L. G. De Vicuna, and M. Castilla, "Hierarchical control of droop-controlled AC and DC microgrids—A general approach toward standardization," *IEEE Trans. Ind. Electron.*, vol. 58, no. 1, pp. 158–172, Jan. 2011.

JIAHUA NI received the B.S. degree in electrical and information engineering from Southwest University, Chongqing, China. He is currently pursuing the Ph.D. degree in electrical engineering with Zhejiang University, Hangzhou, China.

His research interests include PV generation control and renewable energy dispatching.

BO ZHAO (Member, IEEE) received the Ph.D. degree from the Department of Electrical Engineering, Zhejiang University, Hangzhou, China, in 2005. He is currently a Senior Engineer with the State Grid Zhejiang Electric Power Research Institute, Hangzhou. His research interests include distributed generation and microgrids.

ARMAN GOUDARZI received the B.Sc. degree from IAUB, Bushehr, Iran, in 2004, the M.Sc. degree in electrical engineering from Mapúa University, Philippines, in 2012, and the Ph.D. degree in electrical engineering from the University of KwaZulu-Natal, South Africa, in 2017.

He was a Postdoctoral Research Fellow with the College of Electrical, Zhejiang University, Hangzhou, China. In 2018, the Chinese government selected him as an International Talent under the talent introduction program. He has served as a scientific committee member, an editor, and a reviewer for various international journals and conferences. His research interests include power system optimization, demand response programs (DRPs), vehicle-to-grid integration (V2G), electricity markets, intelligent microgrids, integration of renewable energies, and the IoT-enabled smart grids.

YANJUN LI received the Ph.D. degree in control science and engineering from Zhejiang University, Hangzhou, China, in 2001.

From 2001 to 2003, she worked as a Postdoctoral Researcher with Zhejiang University, and City University of Hong Kong, Hong Kong. She was an Associate Professor with Zhejiang University, from 2003 to 2008. She is currently a Professor with the School of Information and Electrical Engineering and the Head of the Key Laboratory of Intelligent Systems, Zhejiang University City College, Hangzhou. Her current research interests include the areas of complex networks, hybrid and nonlinear systems, system modeling and identification, system optimization, and computational intelligence.

JI XIANG (Senior Member, IEEE) received the Ph.D. degree in control science and engineering from Zhejiang University, Hangzhou, China, in 2005.

From 2005 to 2007, he worked as a Postdoctoral Researcher with Zhejiang University and visited the City University of Hong Kong for three months. Under the support of a Gledden Senior Visiting Fellowship, he visited The University of Western Australia, in 2008. From 2013 to 2014, he was a Visiting Scholar with The University of Sydney, Camperdown, NSW, Australia. He is currently a Professor with the Department of System Science and Engineering, Zhejiang University. His research interests include unman surface vehicle, microgrids, multiagent systems, and complex networks.